Cell Reports
Report

Substrate-Activated Conformational Switch on Chaperones Encodes a Targeting Signal in Type III Secretion

Li Chen,[1] Xuanjun Ai,[1] Athina G. Portaliou,[2] Conceicao A.S.A. Minetti,[1] David P. Remeta,[1] Anastassios Economou,[2,3] and Charalampos G. Kalodimos[1,*]
[1]Center of Integrative Proteomics Research and Department of Chemistry & Chemical Biology, Rutgers University, Piscataway, NJ 08854, USA
[2]Institute of Molecular Biology & Biotechnology and Department of Biology, University of Crete, FORTH, PO Box 1385, GR-71110, Iraklio, Crete, Greece
[3]Rega Institute, Katholieke Universiteit Leuven, Molecular Bacteriology Laboratory, Minderbroedersstraat 10, B-3000 Leuven, Belgium
*Correspondence: babis@rutgers.edu
http://dx.doi.org/10.1016/j.celrep.2013.02.025

SUMMARY

The targeting of type III secretion (TTS) proteins at the injectisome is an important process in bacterial virulence. Nevertheless, how the injectisome specifically recognizes TTS substrates among all bacterial proteins is unknown. A TTS peripheral membrane ATPase protein located at the base of the injectisome has been implicated in the targeting process. We have investigated the targeting of the EspA filament protein and its cognate chaperone, CesAB, to the EscN ATPase of the enteropathogenic *E. coli* (EPEC). We show that EscN selectively engages the EspA-loaded CesAB but not the unliganded CesAB. Structure analysis revealed that the targeting signal is encoded in a disorder-order structural transition in CesAB that is elicited only upon the binding of its physiological substrate, EspA. Abrogation of the interaction between the CesAB-EspA complex and EscN resulted in severe secretion and infection defects. Additionally, we show that the targeting and secretion signals are distinct and that the two processes are likely regulated by different mechanisms.

INTRODUCTION

The type III secretion (TTS) system is a multiprotein machinery that has evolved to deliver bacterial virulence proteins directly into eukaryotic cells through an organelle termed the injectisome (Cornelis, 2006; Galán and Wolf-Watz, 2006). The TTS substrates (needle-forming proteins, effectors, and translocators) are targeted to the cytoplasmic base of the injectisome and hierarchically secreted through the channel (Izoré et al., 2011). In the cytosol, TTS substrates are typically found as complexes with their cognate chaperones (Birtalan et al., 2002; Page and Parsot, 2002; Feldman and Cornelis, 2003; Francis, 2010), which have established roles as antiaggregation and stabilizing factors for TTS substrates. It has been hypothesized that chaperones may also act as signals for targeting and hierarchy-determining factors (Birtalan et al., 2002; Lilic et al., 2006; Rodgers et al., 2010; Lara-Tejero et al., 2011).

A key protein in TTS systems is the ATPase (Woestyn et al., 1994; Pallen et al., 2005), a peripheral membrane protein located at the entrance of the injectisome. Biochemical experiments have provided evidence that the TTS ATPase protein, which is ubiquitous to all TTS systems, may serve to recognize and engage the TTS proteins at the injectisome (Gauthier and Finlay, 2003; Akeda and Galán, 2005; Thomas et al., 2005; Boonyom et al., 2010; Cooper et al., 2010). The ATPase is located at the cytoplasmic base of the injectisome and forms a ring structure (Müller et al., 2006) that resembles the F_1F_0-ATPase (Pallen et al., 2006; Imada et al., 2007; Zarivach et al., 2007). The molecular basis for the targeting of TTS substrates to the ATPase remains completely unknown.

We studied this targeting process in enteropathogenic *E. coli* (EPEC), the archetype of a group of pathogens that adhere to host enterocytes via the formation of attaching and effacing lesions and cause extensive host cell cytoskeletal rearrangements (Dean and Kenny, 2009). When secreted, EspA undergoes self-polymerization, thereby forming a long extracellular filamentous extension that coats the needle and connects it to the translocation pore in the eukaryotic plasma membrane, and most likely acts as a molecular conduit for TTS protein translocation (Knutton et al., 1998). EspA has a high tendency to self-oligomerize and, thus, is retained in a monomeric, soluble state in the cytoplasm by forming a complex with the CesAB chaperone (Creasey et al., 2003; Yip et al., 2005).

Here, we show that the homodimeric CesAB chaperone exists in a partially unfolded state and does not interact with the EscN ATPase. In contrast, the formation of the CesAB-EspA chaperone-substrate complex results in a strong affinity for EscN. Structural analysis demonstrated that the binding of EspA to CesAB results in the extensive folding of many regions in the chaperone. The induced structure in one of these regions is specifically recognized by EscN, and it mediates the formation of the ternary EscN-CesAB-EspA complex. Interestingly, a homodimeric CesAB variant designed to adopt a folded structure

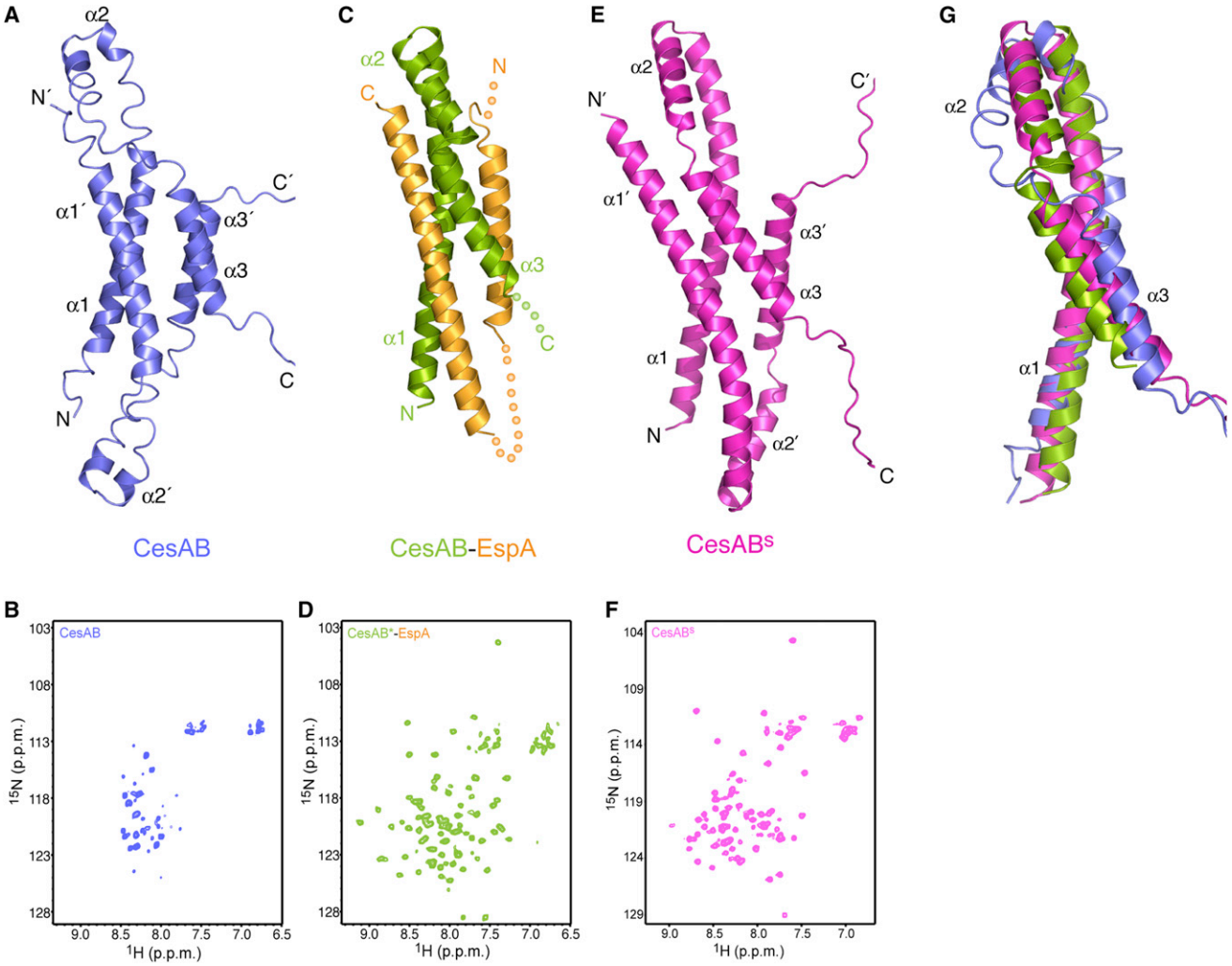

Figure 1. Structures of CesAB, CesAB-EspA, and CesAB^{S}

(A) The solution structure of the homodimeric CesAB, which adopts a molten-globule-like structure in solution (Chen et al., 2011).

(B) The ^{1}H-^{15}N HSQC spectrum of CesAB.

(C) The crystal structure of the heterodimeric CesAB-EspA (Yip et al., 2005). Regions of the proteins that were not crystallographically resolved are represented as dotted lines.

(D) The ^{1}H-^{15}N HSQC spectrum of CesAB-EspA. The CesAB subunit is ^{15}N labeled, whereas the EspA subunit is unlabeled.

(E) The solution structure of the CesAB^{S} variant (D14L-R18D-E20L), as determined in this work.

(F) The ^{1}H-^{15}N HSQC spectrum of CesAB^{S}.

(G) Superposition of the CesAB subunit of CesAB, CesAB-EspA, and CesAB^{S}.

similar to the one induced by EspA binding is capable of interacting with EscN. Amino acid substitutions in the EscN-interacting CesAB region abrogate the targeting of CesAB-EspA to EscN, resulting in severe secretion and infection defects.

RESULTS

The Substrate-Free CesAB Chaperone Does Not Interact with the EscN ATPase

In the absence of its substrate EspA, CesAB exists as a loosely packed, conformationally dynamic homodimer in solution (Chen et al., 2011) (Figures 1A and 1B). CesAB adopts a four-helix bundle structure with each of the subunits in an all-helical conformation consisting of three helices of variable stability (Chen et al., 2011) (Figure 1A). We used nuclear magnetic resonance (NMR) spectroscopy, which is a very sensitive reporter of even transient binding interactions (Takeuchi and Wagner, 2006), to test whether CesAB interacts with the ATPase EscN (Gauthier and Finlay, 2003; Zarivach et al., 2007). For this reason, we prepared full-length EscN, which, as we show here, forms a stable hexamer in solution with stimulated ATPase activity (Figures S2A and S2C). The NMR data show that none of the CesAB resonances are affected by the addition of EscN (Figure S2D), thereby demonstrating that there

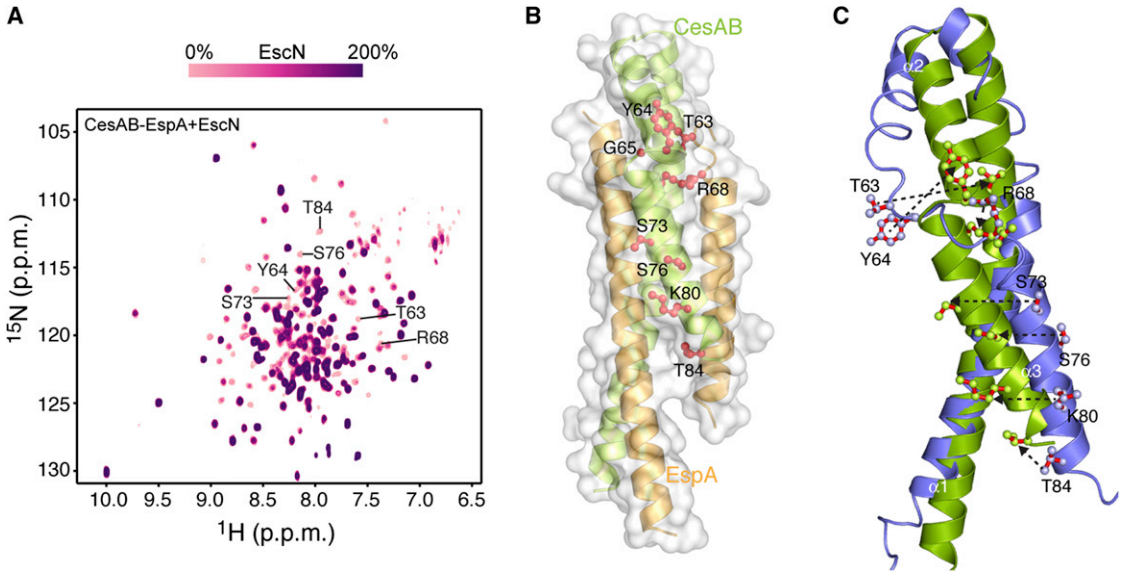

Figure 2. Interaction of CesAB-EspA with EscN

(A) Overlaid ^{1}H-^{15}N HSQC spectra of the titration of U-^{2}H-^{15}N-labeled CesAB-EspA with unlabeled hexameric EscN. Stepwise addition of EscN results in gradual resonance broadening of the interacting residues in CesAB-EspA. Spectra recorded at ten different titration points are overlaid. The CesAB residues most affected by EscN binding are shown. The resonances not affected by EscN binding even at saturating concentrations of EscN are located in flexible regions of EspA that were crystallographically unresolved.

(B) CesAB-EspA residues (shown in red sticks) identified by NMR to be most affected upon binding to EscN. All residues are located in helices α2 and α3 in CesAB.

(C) Superposition of the CesAB subunit of the homodimeric CesAB (blue) and the heterodimeric CesAB-EspA complex (green). The residues identified to mediate the binding of CesAB-EspA to EscN are shown.

is no interaction between CesAB and EscN. Thus, CesAB appears not to be engaged by the injectisome ATPase in its substrate-free form.

The CesAB-EspA Heterodimer Interacts Specifically with the EscN ATPase

The CesAB dimer undergoes subunit exchange to interact with its cognate substrate EspA, resulting in the formation of a 1:1 heterodimeric complex with a molecular mass of ~33 kDa (Figure 1C) (Yip et al., 2005; Chen et al., 2011). The complex forms a four-helix bundle, and each protein contributes two α helices. Interestingly, CesAB, which is poorly folded in the homodimer, acquires a well-folded structure upon binding to EspA (Chen et al., 2011) (Figures 1C and 1D). We used NMR to test the interaction between CesAB-EspA and hexameric EscN. The NMR data show that the addition of EscN causes a very significant effect on a large number of CesAB-EspA resonances (Figures 2A and S2E), indicating the formation of the ternary CesAB-EspA-EscN complex. The dissociation constant (K_d) of the ternary complex, measured by NMR line-shape analysis, is ~3 μM. Thus, the heterodimeric chaperone-substrate complex binds with a significant affinity to the active hexameric state of the injectisome ATPase. Interestingly, no binding was observed between CesAB-EspA and an N-terminal-truncated EscN variant that lacks the first 98 residues ($EscN^{\Delta N}$) and exists in a monomeric state and lacks enzymatic activity (Figures S2B, S2C, and S2F). Thus, EscN has to be in a functional oligomeric state in order to engage the chaperone-substrate complex.

The CesAB-EspA Interaction with EscN Is Mediated by CesAB

To determine the specific residues that mediate the interaction between CesAB-EspA and EscN, we used NMR differential line broadening analysis (Matsuo et al., 1999; Panchal et al., 2003; Zamoon et al., 2005; Takeuchi and Wagner, 2006) (Figure 2A). Because EscN has a large molecular mass (~350 kDa), complex formation with labeled CesAB-EspA results in severe line broadening of the resonances. The broadening effect is related to the chemical shift difference of the CesAB-EspA resonances between the EscN-free and EscN-bound forms. Thus, with the use of this method, the residues in CesAB-EspA that are most affected by the formation of the ternary complex with EscN can be identified.

These results indicate that the residues most affected by EscN binding belong to CesAB. Specifically, Thr63, Tyr64, Arg68, Ser73, Ser76, Lys80, and Thr84 of CesAB experience the strongest effects (Figure 2B). These residues are located in helices α2 and α3 of CesAB in the heterodimer and form a contiguous solvent-exposed surface. The NMR data strongly suggest that this region forms the EscN-binding surface in CesAB-EspA.

It is of interest that CesAB, rather than EspA, appears to be responsible for mediating the binding between CesAB-EspA and EscN. This is surprising, given that CesAB in the homodimer does not interact with EscN (Figure S2D). Structural analysis of the CesAB homodimer and the CesAB-EspA heterodimer shows that the CesAB protomer adopts a similar overall fold; however, in the CesAB homodimer, all three α helices are much shorter,

largely unwound, and more dynamic, in contrast to the CesAB-EspA complex, wherein they are well folded (Figure 1G) (Yip et al., 2005; Chen et al., 2011). Superposition of the CesAB structures of the homodimer and heterodimer shows that the EscN-binding region in CesAB is well formed in the heterodimer but extensively unfolded in the homodimer (Figure 2C).

A Well-Folded CesAB Homodimer Variant Binds Specifically to EscN

The present results suggest that the binding of EspA to CesAB poises CesAB for interaction with EscN by eliciting a disorder-to-order transition that stabilizes the formation of a region that is specifically recognized by EscN (Figure 2C). To test this hypothesis further, we assessed the effect of a CesAB variant that was previously shown to mimic the EspA binding effect and stabilize a well-folded structure of the CesAB homodimer (Chen et al., 2011). Specifically, the D14L-R18D-E20L triple amino acid substitution optimizes coiled-coil interactions at the CesAB helical bundle interface. The stabilized CesAB-D14L-R18D-E20L (henceforth CesAB^{s}) has NMR and circular dichroism (CD) features that are characteristic of a well-folded protein (Figures S1A–S1D).

We determined the solution structure of CesAB^{s} using NMR (Figures 1E, 1F, and S1E and Table S1). CesAB^{s} adopts a structure that is, overall, very similar to that of CesAB (Figures 1G and S1F). However, the packing at the helical bundle in CesAB^{s} is drastically improved (Figure S1E), and CesAB^{s} buried ~3,200 Å^2 in its dimeric interface, in comparison to only ~1,100 Å^2 buried in CesAB.

Interestingly, the CesAB^{s} structure is very similar to the structure that CesAB adopts in the CesAB-EspA heterodimer (Figures 1G and S1G), and all three helices are well folded. Thus, the triple mutant appears to induce the same structural transition to CesAB that EspA binding induces. Most importantly, the EscN binding region is well formed in CesAB^{s}. We used NMR to assess whether CesAB^{s} interacts with EscN. The results clearly show that there is a specific interaction between CesAB^{s} and EscN (Figure S2G), the K_d of the ternary complex being estimated at ~12 μM. The residues most affected upon complex formation are very similar in CesAB^{s} and CesAB-EspA (Figures S1H and S1I). Altogether, the results show that the triple-amino-acid substitution in CesAB^{s} induces an overall structure to CesAB that is similar to the structure induced by EspA binding, and, as a result, EscN specifically recognizes CesAB^{s} and not CesAB.

Disruption of CesAB̄EspA Binding to EscN Gives Rise to Secretion and Functional Defects

To test the binding between CesAB-EspA and EscN, we generated CesAB mutants. Amino acids in the region identified to mediate the interaction (Figure 2B) were mutated, and their effect on the formation of the CesAB-EspA-EscN ternary complex was assessed by NMR and in vivo secretion assays (Figure 3). The data showed that substitutions at Glu60, Tyr64, Arg68, and Lys69 substantially decrease the affinity of CesAB-EspA for EscN. For example, the K_d of CesAB-EspA-Y64A-R68A for EscN is larger than 80 μM, which is larger than that of CesAB-EspA by more than a factor of 20. As a result of the much weaker interaction between the mutated CesAB-EspA and EscN, secretion of EspA decreases substantially (Figure 3B). In addition, infection of HeLa cells by EPEC strains carrying *cesAB* mutated genes causes minimal actin polymerization and pedestal formation, indicating the defective secretion of TTS effectors (Figures 3C and 3D). It should be noted that, in the absence of EscN, EspA is not secreted (Figure S3). Collectively, these results provide strong evidence that the efficient targeting of CesAB-EspA to EscN is required for EspA secretion.

Targeting and Secretion Signals Are Distinct

It was previously shown that the first ~20 N-terminal residues of EspA bear a secretion signal for EspA, given that the deletion of this region resulted in EspA secretion defects (Munera et al., 2010). NMR analysis of the interaction of CesAB-EspA with EscN (Figure 2A) shows that the N-terminal region of EspA does not participate in the binding interaction. To corroborate this further, we characterized the interaction of the isolated N-terminal region of EspA (EspA$^{1–34}$) with EscN by NMR. The data showed that this region indeed does not interact with EscN (Figure S2J). Additional evidence that the region of EspA carrying the secretion signal does not participate in binding to EscN was provided by NMR analysis of CesAB-EspA$^{\Delta 29}$, a variant comprising an N-truncated EspA lacking the first 29 residues. CesAB-EspA$^{\Delta 29}$ retains the same fold and structure as the full-length CesAB-EspA (Figure S2K) but is fully engaged by EscN (Figure S2L). Thus, although EspA is targeted to the ATPase by means of CesAB, there are regions in EspA that control its secretion, most likely during a downstream process following the targeting of EspA at the injectisome. These results demonstrate that the targeting and secretion signals are distinct and that the two processes are likely regulated by different mechanisms.

DISCUSSION

The targeting of TTS secreted proteins at the injectisome is the first crucial step in a process that ultimately results in the secretion of needle and translocator proteins or the translocation of effectors into the eukaryotic cell. The cytosolic basal structure of the injectisome is capable of discerning the TTS substrates from all the other bacterial proteins; yet, the molecular basis for this process remains poorly understood. Here, we have identified the targeting signal in the *EPEC* CesAB-EspA chaperone-substrate system. We show that the signal is encoded in a conformational switch in the chaperone that is induced only upon the binding of the physiological substrate (Figure 4). Our results clearly demonstrate that chaperones contain targeting signals and, thus, act to usher bound substrates to the injectisome.

Several studies have focused on identifying the so-called secretion signal, that is, the region of the TTS substrate that controls its secretion (Mota et al., 2005). The results have suggested, in certain cases, that specific sequences in the N-terminal region of effectors and translocators constitute the secretion signal (Sory et al., 1995; Lloyd et al., 2001; Amer et al., 2011), whereas, in other cases, it has been suggested

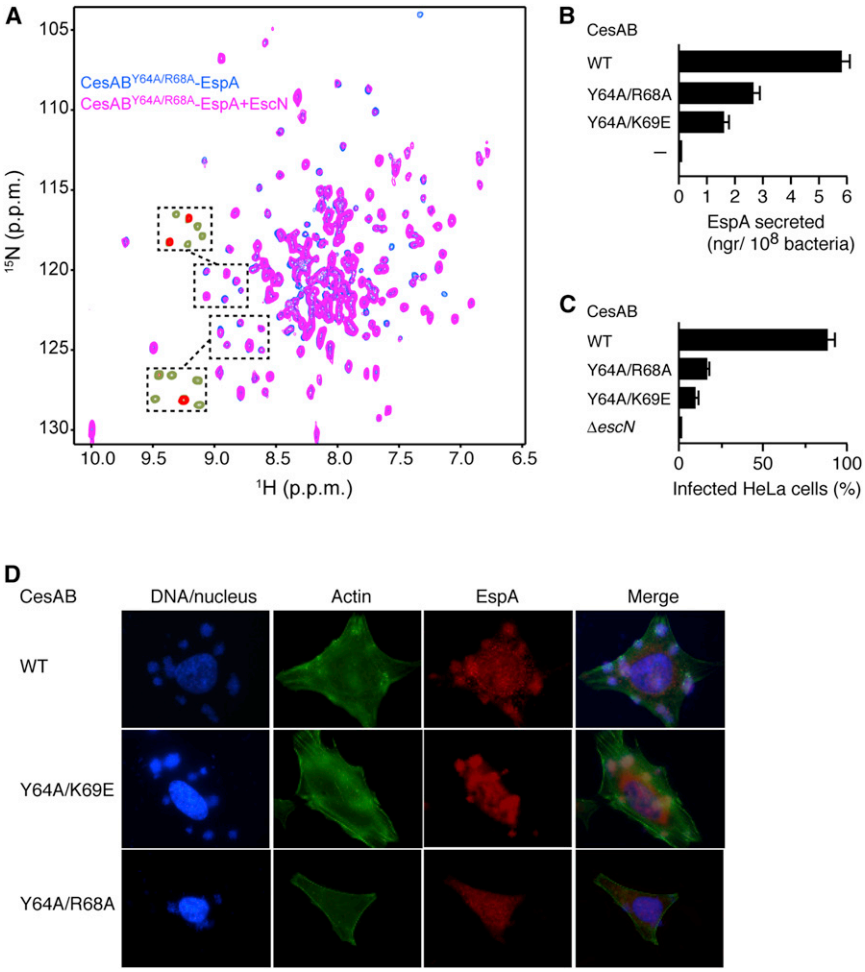

Figure 3. Disruption of CesAB-EspA Binding to EscN Gives Rise to Secretion and Functional Defects

(A) The effect of the Y64A-R68A substitution on the interaction of CesAB-EspA with EscN. Overlaid ^{1}H-^{15}N HSQC spectra of CesAB$^{Y64A-R68A}$-EspA in the absence (blue) and presence (magenta) of EscN. In comparison to wild-type CesAB-EspA binding to EscN, the NMR data indicate a significant decrease in the affinity of the ternary complex (K_d is larger than 80 μM). The boxed areas show the corresponding regions of the spectra of CesAB-EspA (green) superimposed on the spectra of its complex with EscN (red). Whereas the majority of the peaks are broadened beyond detection in the CesAB-EspA-EscN complex, they are still present at a substantial intensity in the CesAB$^{Y64A-R68A}$-EspA-EscN complex.

(B) In vivo secretion of EspA from EPECΔ*cesAB* strains complemented with pASK-IBA7 plasmids expressing wild-type or mutated CesAB. The graph reports the total amount of EspA secreted in 90 min after CesAB expression. Errors were calculated from a triplicate experiment.

(C) In vivo infection of HeLa cells from EPECΔ*cesAB* or EPECΔ*escN* strains complemented with pASK-IBA7 plasmids expressing wild-type or mutated CesAB. The graph reports the percentage of HeLa cells infected after being inoculated with bacteria for 90 min. Errors were calculated from a triplicate experiment.

(D) The infection of HeLa cells by bacterial EPECΔcesAB strains complemented with plasmids expressing wild-type or mutant CesAB. The results show very little actin pedestal formation, indicating uninfected HeLa cells, after being inoculated with bacteria for 90 min.

that the secretion signal is encoded in the messenger RNA sequence (Anderson and Schneewind, 1997; Ramamurthi and Schneewind, 2005). However, secretion is a complex process, and targeting is just the first step of it. Indeed, here, we demonstrate that the targeting and secretion of the CesAB-EspA chaperone-substrate system are controlled by different signals: the targeting signal is encoded in the chaperone (CesAB), whereas the secretion signal is located in the N-terminal region of EspA (Munera et al., 2010). This region of EspA is not required for binding to the ATPase but is required for its ultimate secretion, a process that occurs after the chaperone-substrate complex has been engaged by the injectisome.

The TTS ATPase is conserved in all TTS systems and is thought to play important roles in both engaging TTS substrates and in the secretion process (Galán, 2008). Our results show that, in the EPEC system, the EscN ATPase functions as a docking platform for chaperone-substrate complexes. The interactions are functional, given that the abrogation of binding causes severe secretion and infection defects. However, it is likely that additional proteins of the cytosolic basal body of the injectisome may also function as docking points for TTS substrates (Diepold et al., 2012).

EXPERIMENTAL PROCEDURES

Protein Preparation

The *cesAB* and *espA* genes encoding the wild-type CesAB (B7UMC4_ECO27) and the wild-type EspA (B7UM94_ECO27) were isolated and cloned as described previously (Chen et al., 2011). The ATPase *escN* encoding EscN (B7UMA6_ECO27) was isolated by PCR from cosmid pCVD462 (a gift from J.B. Kaper) derived from the locus of enterocyte effacement of E2348/69 cloned into pCVD551 (McDaniel and Kaper, 1997) and were finally cloned into pET16b. The mutants were constructed by site-directed mutagenesis with the use of PfuUltra High-Fidelity DNA Polymerase (Quick-Change; Stratagene). The constructs were transformed in BL21(DE3) cells and grown at 37°C, and protein synthesis was induced by the addition of 0.5 mM of IPTG at A_{600} ~0.4. Isotopically labeled samples for NMR studies were prepared as described previously (Gelis et al., 2007; Popovych et al., 2009). All protein samples were purified over a nickel-chelating Sepharose column (GE Healthcare) followed by a Superdex 75 size exclusion column (GE Healthcare).

Differential Line Broadening NMR Experiments

Because EscN has a large molecular mass (~350 kDa), complex formation with labeled CesAB-EspA resulted in severe line broadening of the resonances. The broadening effect depends on the chemical shift difference of the CesAB-EspA resonances between the EscN-free and EscN-bound forms (Matsuo et al., 1999). Thus, with the use of this method, the residues in CesAB-EspA that are most affected by the formation of the ternary complex with EscN

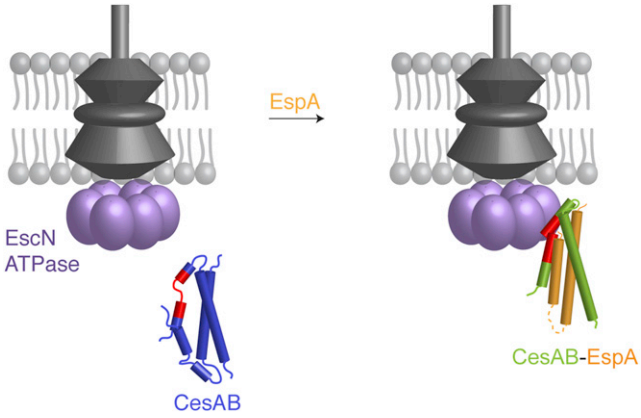

Figure 4. Targeting of CesAB-EspA to the ATPase
Although CesAB carries the targeting signal (shown in red), this is presented to EscN only when EspA is bound to CesAB by means of an induced conformational switch on CesAB. As a result, EscN recognizes the restructured CesAB region and engages the CesAB-EspA complex.

can be identified. The experiments were performed with a concentration of ^{15}N-labeled CesAB-EspA complex fixed at 0.2 mM while an increasing amount of unlabeled EscN was titrated. The concentration ratio of CesAB-EspA complex to the ATPase EscN varied from 0.2 to 2 mM. The intensity of CesAB-EspA resonances as a function of EscN concentration was measured in 2D ^{1}H-^{15}N HSQC spectra.

ATPase Activity Measured via Isothermal Titration Calorimetry

ATPase activity assays were performed via isothermal titration calorimetry on a VP-ITC MicroCalorimeter (GE Healthcare) employing a multi-injection analysis protocol (Todd and Gomez, 2001; Bianconi, 2007). This methodology is based on the observed proportionality between the rate of reaction (v) and thermal power (dq/dt) generated upon titration of discrete substrate aliquots into an enzyme solution. The rate of product formation is determined according to the following relation:

$$v = \frac{dq}{dt}\frac{1}{V\Delta H_{app}}$$

where V represents the sample cell volume and ΔH_{app} corresponds to the molar reaction enthalpy. ATPase activity was monitored calorimetrically at 25°C in a buffer comprised of 50 mM HEPES, 100 mM NaCl, 5 mM $MgCl_2$, and 5.0 mM β-mercaptoethanol adjusted to pH 7.5. In a typical calorimetric assay, the reaction rate is monitored by titrating successive microliter aliquots of ATP substrate into the sample cell containing EscN. The thermal power is monitored for 60 s upon each substrate injection under a constant stirring rate of 250 rpm. Assuming that the reaction proceeds via a steady-state mode in which [substrate] ≫ [enzyme], the differential power upon each addition of substrate represents the maximal enzyme reaction rate and is characterized by an exothermic heat that remains nearly constant until the next injection. The thermal power data monitoring ATP hydrolysis is converted to the turnover rate (mM s^{-1}) and plotted as a function of substrate concentration. The reaction profiles depicted in Figure S2C employ initial substrate (ATP) and enzyme (EscN) concentrations of 2.5 and 0.006 mM, respectively.

In Vivo Secretion from EPEC Strains and Infection of HeLa Cells

The assays were performed as described previously. Details can be found in Extended Experimental Procedures.

ACCESSION NUMBERS

The atomic coordinates for CesAB^{s} have been deposited in the Protein Data Bank at accession number 1M1N.

SUPPLEMENTAL INFORMATION

Supplemental Information includes Extended Experimental Procedures and three figures and can be found with this article online at http://dx.doi.org/10.1016/j.celrep.2013.02.025.

LICENSING INFORMATION

ACKNOWLEDGMENTS

This work was supported by the National Institutes of Health (grant AI094623 to C.G.K.), the Operational Programme "Competitiveness and Entrepreneurship" (OPCE II-EPAN II), the National Strategic Reference Framework (NSRF 2007-2013 and 09SYN-11-902 to A.E.), and a Research Excellence Grant from the Greek General Secretariat of Research (1473-Nonaco to A.E.).

Received: December 24, 2012
Revised: January 27, 2013
Accepted: February 22, 2013
Published: March 21, 2013

REFERENCES

Akeda, Y., and Galán, J.E. (2005). Chaperone release and unfolding of substrates in type III secretion. Nature *437*, 911–915.

Amer, A.A., Åhlund, M.K., Bröms, J.E., Forsberg, A., and Francis, M.S. (2011). Impact of the N-terminal secretor domain on YopD translocator function in Yersinia pseudotuberculosis type III secretion. J. Bacteriol. *193*, 6683–6700.

Anderson, D.M., and Schneewind, O. (1997). A mRNA signal for the type III secretion of Yop proteins by Yersinia enterocolitica. Science *278*, 1140–1143.

Bianconi, M.L. (2007). Calorimetry of enzyme-catalyzed reactions. Biophys. Chem. *126*, 59–64.

Birtalan, S.C., Phillips, R.M., and Ghosh, P. (2002). Three-dimensional secretion signals in chaperone-effector complexes of bacterial pathogens. Mol. Cell *9*, 971–980.

Boonyom, R., Karavolos, M.H., Bulmer, D.M., and Khan, C.M.A. (2010). Salmonella pathogenicity island 1 (SPI-1) type III secretion of SopD involves N- and C-terminal signals and direct binding to the InvC ATPase. Microbiology *156*, 1805–1814.

Chen, L., Balabanidou, V., Remeta, D.P., Minetti, C.A.S.A., Portaliou, A.G., Economou, A., and Kalodimos, C.G. (2011). Structural instability tuning as a regulatory mechanism in protein-protein interactions. Mol. Cell *44*, 734–744.

Cooper, C.A., Zhang, K., Andres, S.N., Fang, Y., Kaniuk, N.A., Hannemann, M., Brumell, J.H., Foster, L.J., Junop, M.S., and Coombes, B.K. (2010). Structural and biochemical characterization of SrcA, a multi-cargo type III secretion chaperone in Salmonella required for pathogenic association with a host. PLoS Pathog. *6*, e1000751.

Cornelis, G.R. (2006). The type III secretion injectisome. Nat. Rev. Microbiol. *4*, 811–825.

Creasey, E.A., Friedberg, D., Shaw, R.K., Umanski, T., Knutton, S., Rosenshine, I., and Frankel, G. (2003). CesAB is an enteropathogenic Escherichia coli chaperone for the type-III translocator proteins EspA and EspB. Microbiology *149*, 3639–3647.

Dean, P., and Kenny, B. (2009). The effector repertoire of enteropathogenic E. coli: ganging up on the host cell. Curr. Opin. Microbiol. *12*, 101–109.

Diepold, A., Wiesand, U., Amstutz, M., and Cornelis, G.R. (2012). Assembly of the Yersinia injectisome: the missing pieces. Mol. Microbiol. *85*, 878–892.

Feldman, M.F., and Cornelis, G.R. (2003). The multitalented type III chaperones: all you can do with 15 kDa. FEMS Microbiol. Lett. *219*, 151–158.

Francis, M.S. (2010). Type III Secretion Chaperones: A Molecular Toolkit for All Occasions (Handbook of Molecular Chaperones: Roles, Structures and Mechanisms), 79–147.

Galán, J.E. (2008). Energizing type III secretion machines: what is the fuel? Nat. Struct. Mol. Biol. *15*, 127–128.

Galán, J.E., and Wolf-Watz, H. (2006). Protein delivery into eukaryotic cells by type III secretion machines. Nature *444*, 567–573.

Gauthier, A., and Finlay, B.B. (2003). Translocated intimin receptor and its chaperone interact with ATPase of the type III secretion apparatus of enteropathogenic Escherichia coli. J. Bacteriol. *185*, 6747–6755.

Gelis, I., Bonvin, A.M.J.J., Keramisanou, D., Koukaki, M., Gouridis, G., Karamanou, S., Economou, A., and Kalodimos, C.G. (2007). Structural basis for signal-sequence recognition by the translocase motor SecA as determined by NMR. Cell *131*, 756–769.

Imada, K., Minamino, T., Tahara, A., and Namba, K. (2007). Structural similarity between the flagellar type III ATPase FliI and F1-ATPase subunits. Proc. Natl. Acad. Sci. USA *104*, 485–490.

Izoré, T., Job, V., and Dessen, A. (2011). Biogenesis, regulation, and targeting of the type III secretion system. Structure *19*, 603–612.

Knutton, S., Rosenshine, I., Pallen, M.J., Nisan, I., Neves, B.C., Bain, C., Wolff, C., Dougan, G., and Frankel, G. (1998). A novel EspA-associated surface organelle of enteropathogenic Escherichia coli involved in protein translocation into epithelial cells. EMBO J. *17*, 2166–2176.

Lara-Tejero, M., Kato, J., Wagner, S., Liu, X., and Galán, J.E. (2011). A sorting platform determines the order of protein secretion in bacterial type III systems. Science *331*, 1188–1191.

Lilic, M., Vujanac, M., and Stebbins, C.E. (2006). A common structural motif in the binding of virulence factors to bacterial secretion chaperones. Mol. Cell *21*, 653–664.

Lloyd, S.A., Forsberg, A., Wolf-Watz, H., and Francis, M.S. (2001). Targeting exported substrates to the Yersinia TTSS: different functions for different signals? Trends Microbiol. *9*, 367–371.

Matsuo, H., Walters, K., Teruya, K., Tanaka, T., Gassner, G., Lippard, S., Kyogoku, Y., and Wagner, G. (1999). Identification by NMR spectroscopy of residues at contact surfaces in large, slowly exchanging macromolecular complexes. J. Am. Chem. Soc. *121*, 9903–9904.

McDaniel, T.K., and Kaper, J.B. (1997). A cloned pathogenicity island from enteropathogenic Escherichia coli confers the attaching and effacing phenotype on E. coli K-12. Mol. Microbiol. *23*, 399–407.

Mota, L.J., Sorg, I., and Cornelis, G.R. (2005). Type III secretion: the bacteria-eukaryotic cell express. FEMS Microbiol. Lett. *252*, 1–10.

Müller, S.A., Pozidis, C., Stone, R., Meesters, C., Chami, M., Engel, A., Economou, A., and Stahlberg, H. (2006). Double hexameric ring assembly of the type III protein translocase ATPase HrcN. Mol. Microbiol. *61*, 119–125.

Munera, D., Crepin, V.F., Marches, O., and Frankel, G. (2010). N-terminal type III secretion signal of enteropathogenic Escherichia coli translocator proteins. J. Bacteriol. *192*, 3534–3539.

Page, A.L., and Parsot, C. (2002). Chaperones of the type III secretion pathway: jacks of all trades. Mol. Microbiol. *46*, 1–11.

Pallen, M.J., Beatson, S.A., and Bailey, C.M. (2005). Bioinformatics analysis of the locus for enterocyte effacement provides novel insights into type-III secretion. BMC Microbiol. *5*, 9.

Pallen, M.J., Bailey, C.M., and Beatson, S.A. (2006). Evolutionary links between FliH/YscL-like proteins from bacterial type III secretion systems and second-stalk components of the FoF1 and vacuolar ATPases. Protein Sci. *15*, 935–941.

Panchal, S.C., Kaiser, D.A., Torres, E., Pollard, T.D., and Rosen, M.K. (2003). A conserved amphipathic helix in WASP/Scar proteins is essential for activation of Arp2/3 complex. Nat. Struct. Biol. *10*, 591–598.

Popovych, N., Tzeng, S.-R., Tonelli, M., Ebright, R.H., and Kalodimos, C.G. (2009). Structural basis for cAMP-mediated allosteric control of the catabolite activator protein. Proc. Natl. Acad. Sci. USA *106*, 6927–6932.

Ramamurthi, K.S., and Schneewind, O. (2005). A synonymous mutation in Yersinia enterocolitica yopE affects the function of the YopE type III secretion signal. J. Bacteriol. *187*, 707–715.

Rodgers, L., Mukerjea, R., Birtalan, S., Friedberg, D., and Ghosh, P. (2010). A solvent-exposed patch in chaperone-bound YopE is required for translocation by the type III secretion system. J. Bacteriol. *192*, 3114–3122.

Sory, M.P., Boland, A., Lambermont, I., and Cornelis, G.R. (1995). Identification of the YopE and YopH domains required for secretion and internalization into the cytosol of macrophages, using the cyaA gene fusion approach. Proc. Natl. Acad. Sci. USA *92*, 11998–12002.

Takeuchi, K., and Wagner, G. (2006). NMR studies of protein interactions. Curr. Opin. Struct. Biol. *16*, 109–117.

Thomas, N.A., Deng, W., Puente, J.L., Frey, E.A., Yip, C.K., Strynadka, N.C.J., and Finlay, B.B. (2005). CesT is a multi-effector chaperone and recruitment factor required for the efficient type III secretion of both LEE- and non-LEE-encoded effectors of enteropathogenic Escherichia coli. Mol. Microbiol. *57*, 1762–1779.

Todd, M.J., and Gomez, J. (2001). Enzyme kinetics determined using calorimetry: a general assay for enzyme activity? Anal. Biochem. *296*, 179–187.

Woestyn, S., Allaoui, A., Wattiau, P., and Cornelis, G.R. (1994). YscN, the putative energizer of the Yersinia Yop secretion machinery. J. Bacteriol. *176*, 1561–1569.

Yip, C.K., Finlay, B.B., and Strynadka, N.C.J. (2005). Structural characterization of a type III secretion system filament protein in complex with its chaperone. Nat. Struct. Mol. Biol. *12*, 75–81.

Zamoon, J., Nitu, F., Karim, C., Thomas, D.D., and Veglia, G. (2005). Mapping the interaction surface of a membrane protein: unveiling the conformational switch of phospholamban in calcium pump regulation. Proc. Natl. Acad. Sci. USA *102*, 4747–4752.

Zarivach, R., Vuckovic, M., Deng, W., Finlay, B.B., and Strynadka, N.C.J. (2007). Structural analysis of a prototypical ATPase from the type III secretion system. Nat. Struct. Mol. Biol. *14*, 131–137.